Environ Sci Pollut Res (2015) 22:7590–7599
DOI 10.1007/s11356-014-3880-x

RESEARCH ARTICLE

Aberration of mitosis by hexavalent chromium in some Fabaceae members is mediated by species-specific microtubule disruption

Eleftherios P. Eleftheriou · Vasiliki A. Michalopoulou · Ioannis-Dimosthenis S. Adamakis

Received: 11 July 2014 / Accepted: 17 November 2014 / Published online: 25 January 2015

Abstract Because the detrimental effects of chromium (Cr) to higher plants have been poorly investigated, the present study was undertaken to verify the toxic attributes of hexavalent chromium [Cr(VI)] to plant mitotic microtubules (MTs), to determine any differential disruption of MTs during mitosis of taxonomically related species and to clarify the relationship between the visualized chromosomal aberrations and the Cr(VI)-induced MT disturbance. For this purpose, 5-day-old uniform seedlings of *Vicia faba*, *Pisum sativum*, *Vigna sinensis* and *Vigna angularis*, all belonging to the Fabaceae family, were exposed to 250 μM Cr(VI) supplied as potassium dichromate ($K_2Cr_2O_7$) for 24, 72 and 120 h and others in distilled water serving as controls. Root tip samples were processed for tubulin immunolabelling (for MT visualization) and DNA fluorescent staining (for chromosomal visualization). Microscopic preparations of cell squashes were then examined and photographed by confocal laser scanning microscopy (CLSM). Cr(VI) halted seedling growth turning roots brown and necrotic. Severe chromosomal abnormalities and differential disturbance of the corresponding MT arrays were found in all mitotic phases. In particular, in *V. faba* MTs were primarily depolymerized and replaced by atypical tubulin conformations, whereas in *P. sativum*, *V. sinensis* and *V. angularis* they became bundled in a time-dependent manner. In *P. sativum*, the effects were milder compared to those of the other species, but in all cases MT disturbance adversely affected the proper aggregation of chromosomes on the metaphase plate, their segregation at anaphase and organization of the new nuclei at telophase. Cr(VI) is very toxic to seedling growth. The particular effect depends on the exact stage the cell is found at the time of Cr(VI) entrance and is species-specific. Mitotic MT arrays are differentially deranged by Cr(VI) in the different species examined, even if they are taxonomically related, while their disturbance underlies chromosomal abnormalities. Results furthermore support the view that MTs may constitute a reliable, sensitive and universal subcellular marker for monitoring heavy metal toxicity.

Keywords Chromosomal aberration · Fabaceae · Hexavalent chromium · Mitotic microtubule arrays disruption · Species-specific toxicity

Responsible editor: Philippe Garrigues.

E. P. Eleftheriou (✉) · V. A. Michalopoulou · I.-D. S. Adamakis
Department of Botany, School of Biology, Aristotle University of Thessaloniki, 541 24 Thessaloniki, Greece
e-mail: eelefth@bio.auth.gr

Introduction

Microtubules (MTs) are essential components of the plant cytoskeleton and exert fundamental functions in cell division, elongation and differentiation. Normally, plant cells develop conspicuous MT arrays that assemble at distinct stages of the cell cycle. During mitosis, MTs form three principle arrays [preprophase band (PPB), mitotic spindle, phragmoplast] corresponding respectively to successive mitotic phases (prophase, metaphase/anaphase, telophase) and participate in diverse yet fundamental activities as the definition of the division site, the segregation of daughter chromosomes and the directed transport of cell plate vesicles (Hepler and Hush 1996). In higher plants, a transient system of MTs usually appears around the metatelophasic nuclei, to be succeeded in interphase by an array of cortical MTs (Wick 1985). The ability of MTs to rearrange rapidly into distinct arrays derives largely from their dynamic nature that allows quick depolymerization and repolymerization (van der Vaart et al. 2009). It is then consequent to assume that any adverse interference in MT turnover is expected to induce dramatic effects to their integrity and functioning.

A range of chemical compounds are well known to either depolymerize (e.g. colchicine, oryzalin) or stabilize (e.g. taxol) MTs, both cases resulting in severe functional disorder due to loss of MT dynamic properties (Morejohn 1991). Moreover, the anti-MT attributes of toxic heavy metals and the impact on MT-related functions in plant cells have also attracted the attention of researchers. For example, cadmium disturbed dramatically the MT cytoskeleton of root meristematic apical cells of *Pisum sativum* (Fusconi et al. 2007) and *Allium sativum* (Xu et al. 2009), whereas aluminium deranged the mechanisms controlling the organization of MT cytoskeleton and tubulin polymerization in *Triticum turgidum*, thus disrupting all mitotic phases and cytokinesis (Frantzios et al. 2000, 2001). Negative effects on MT integrity and function were also reported for lead (Eun et al. 2000; Liu et al. 2009), copper (Liu et al. 2009), the metalloid arsenic (Dho et al. 2010) and tungsten (Adamakis et al. 2008, 2010a, b, 2011).

A less studied metal for its toxicity to the plant cell cytoskeleton is chromium (Cr). Being one of the most abundant metals in the earth's crust and possessing some unique physical properties (lustrous, colourful compounds, high corrosion resistance, hardness), Cr is widely used on a large industrial scale including metallurgy, electroplating, tannery, cement plants, alloying, manufacturing of textile dyes, paints and pigments, wood preservation and paper production. These anthropogenic activities have consequently increased environmental contamination, posing serious concerns for human health hazards and downgrading of the biota (Hu et al. 2013; Liu et al. 2013). Chromium exists in several oxidation states, the most stable and common being the trivalent [Cr(III)] and hexavalent [Cr(VI)] ones (Kimbrough et al. 1999). Both forms at high concentrations are toxic, with Cr(VI) considered to be the most harmful because of its high oxidizing potential, solubility and mobility in soil/water systems and living organisms (Oliveira 2012).

Of local interest is the Asopos River case in Central Greece. Due to intense industrialization of the river's drainage basin during the last decades, high amounts of Cr(VI) were found in the river's water and mud, in surface sediments along the river and in the seabed mud at the river's estuarine (Botsou et al. 2011; Economou-Eliopoulos et al. 2011). Cr(VI) concentrations determined in some areas of the river's drainage basin ranged from 13 to 212 μg L^{-1} (median 58 μg L^{-1}) (Tziritis et al. 2012), thus exceeding the permissible limit for human consumption (50 μg L^{-1} for total Cr) established by the 98/83 EC European Union Directive (EC 1998), raising the concern of local civil societies for drinking water and agricultural crop pollution. However, measurement of Cr(VI) concentration and of other trace elements in specific crops (carrots, onions and potatoes) produced in the region, revealed that, though elevated amounts were found compared to controls, the mean daily intake for an average consumption pattern was generally well below the Allowable Daily Intakes (Kirkillis et al. 2012).

The great majority of studies in plants refer to Cr uptake, accumulation, translocation, the potentiality of phytoremediation, its effects on seed germination, root, stem and leaf growth, yield, photosynthesis, membrane structure, mineral nutrition and enzymes (Oliveira 2012; Singh et al. 2013). Moreover, a large number of papers have provided ample evidence of the cytotoxic and genotoxic attributes of Cr, especially of Cr(VI), to diverse plant species including *Vicia faba* (Wang 1999; Qian 2004), *Brassica napus* (Labra et al. 2004), *P. sativum* (Rodriguez et al. 2011), *Allium cepa* (Eleftheriou et al. 2012), *Lens culinaris* (Eleftheriou et al. 2013) and *Hordeum vulgare* (Truta et al. 2014). In meristematic tissues, Cr(VI) caused profound disorders to mitosis including chromosome bridging, stickiness, fragmentation, uncoiling, looping and lagging, and micronuclei formation (Knasmüller et al. 1998; Wang 1999; Qian 2004; Truta et al. 2014). However, few studies have advanced beyond the macro- and microscopically visible effects of Cr(VI) toxicity (Vázquez et al. 1987; Speranza et al. 2007, 2009) and even fewer correlated the visible chromosomal aberrations with the underlying microtubule cytoskeleton (Eleftheriou et al. 2012, 2013).

Therefore, the objectives of the present study were to: (i) determine the detrimental effects of Cr(VI) to plant mitotic MTs, (ii) detect any differential disruption of MTs during mitosis of taxonomically related species, and (iii) clarify the relationship between the Cr(VI)-induced MT disturbance with the visualized chromosomal aberrations. For this purpose, four plant species of the Fabaceae family were studied by confocal laser scanning microscopy (CLSM) after immunolocalization of MTs and fluorescent staining of DNA.

Materials and methods

Plant material and preliminary experiments

Seedlings of *V. faba* (broad bean), *P. sativum* (pea), *Vigna sinensis* (blackeyed pea) and *V. angularis* (azuki bean), all belonging to the Fabaceae family, were used as the experimental material. Seeds were purchased from an agricultural local market except for *V. angularis* which were a generous offer from Dr. Takahiro Hamada (Kyoto University, Japan). Seedlings were raised in distilled water for 4 to 5 days at room temperature (~22 °C) in the dark. To study the macroscopic effects of Cr toxicity, seedlings of all investigated species were exposed at room temperature to 250 μM Cr(VI) supplied as potassium dichromate ($K_2Cr_2O_7$) for 24 and 72 h and compared to untreated ones having the same root length at the beginning of the experiment (day zero). For *V. faba* and *P. sativum*, prolonged treatments up to 120 h have also been conducted. This concentration was adopted taking into

account previous studies in *A. cepa* and *L. culinaris* (Eleftheriou et al. 2012, 2013). Control seedlings were placed on distilled water under the same conditions.

Microtubule immunolocalization and chromosome visualization

To investigate the presumed microscopic disturbance of the cell cycle and of the MT cytoskeleton, seedlings were exposed to 250 μM Cr(VI) for 24 h and studied comparatively to untreated ones. Imaging of *a*-tubulin (MTs) and DNA (chromosomes) was carried out as previously described (Eleftheriou et al. 2012, 2013). Microtubule immunolocalization in squashed root tip cells was carried out with a rat anti-α-tubulin antibody (YOL 1/34, Serotec) or a mouse anti-α-tubulin antibody (DM1A, Santa Cruz), diluted 1:80 in PEM buffer (50 mM PIPES, 5 mM EGTA, 5 mM $MgSO_4 \cdot 7H_2O$, pH 6.8). After washing with PEM, the cells were incubated respectively with 1:80 FITC-anti-rat or FITC-anti-mouse in the same buffer for 3 h at room temperature, followed by 1 h at 37 °C. DNA was counterstained with 3 μg ml^{-1} propidium iodide in PEM. Finally, the coverslips were mounted in an anti-fade solution of 0.1 % *p*-phenylenediamine and 2:1 (*v*/*v*) glycerol/PEM.

The specimens were then examined with a Nikon D-Eclipse C1 confocal laser scanning microscope (CLSM), with an optical sectioning step of 0.30 or 0.50 μm depending on the species examined as already described by Eleftheriou et al. (2013).

Results

Cr(VI) effects to seedling growth

Macroscopic images of all species investigated showed an inhibition of root growth in Cr-treated seedlings over the control, evident even after 24 h of exposure (Fig. 1).[1] In 72 and 120 h of Cr treatment, the roots remained short, became dark brown and occasionally obtained a hook-like bending at the root tip. While the control seedlings continued growing and initiated the formation of lateral roots, the Cr-treated ones succeeded only to emerge their shoots, which in general remained much shorter than the controls (Fig. 1). In some seedlings, a very poor lateral rooting was observed.

[1] The confocal laser scanning microscopy (CLSM) figures were obtained from seedlings treated with 250 μM Cr(VI) for 24 h, except for Fig. 5g that was treated for 72 h, and of equivalent controls. All CLSM figures are projections of serial optical sections unless otherwise stated. Both tubulin (microtubules—MTs) immunolocalization (green) and DNA staining (red) are shown, either single or merged. When figures of the same cell are used, they are identified by the same letter and numbered consecutively. Cells are placed with their longitudinal axis vertical in accordance with the normal orientation of the root.

Microscopic effects

Vicia faba

Interphase cells of untreated roots of *V. faba* contained numerous MTs parallel to each other and transversely aligned to the longitudinal axis of the root (Fig. 2a). In Cr-treated roots, the cortical MTs appeared sparse and oriented in random (Fig. 2b). Preprophase and prophase control cells developed a well-organized preprophase band (PPB) of MTs located at the cell periphery encircling symmetrically the nucleus, the latter being encaged by a perinuclear system of MTs (Fig. 2c). In the Cr-treated prophase cells, the PPB consisted of poorly arranged MTs, while the prophase perinuclear system did not develop (Fig. 2d). Top images of prophase control cells displayed a polar cap of radiating MTs enshrouding the nucleus and a girdle of PPB of MTs at the cell cortex encircling the nucleus (Fig. $2e_1$), which contained highly condensed chromosomes (Fig. $2e_2$). After exposure to Cr(VI), the prometaphase spindle was disordered and consisted of random thick masses of tubulin intermingled with the chromosomes (Fig. $2f_1$, $_2$).

The metaphase spindle of control cells formed two mirrored moieties extending among the accumulated chromosomes in the equatorial plane of the metaphase plate (Fig. $3a_1$, $_2$). In the Cr-treated metaphase cells the spindle appeared asymmetrical and consisted of short dense tubulin bundles (Fig. $3b_1$), whereas the chromosomes were not aggregated properly on the metaphase plate (Fig. $3b_2$). The anaphase spindle of untreated cells appeared quite symmetrical composed of two shortened groups of MTs (Fig. $3c_1$), reflecting the daughter chromosomes being well separated and drawn to opposing directions to the poles (Fig. $3c_2$). The corresponding spindle MTs of Cr-treated anaphase cells formed compact atypical conformations leaving a clear-cut space between them (Fig. $3d_1$), while chromosomes remained unseparated and entangled in the cell centre, displaying several projecting arms (Fig. $3d_2$).

Pisum sativum

Defects in Cr-treated meristematic root tips of *P. sativum* were evident in all mitotic phases compared to control ones (Fig. 4), yet they were milder than those of *V. faba* (cf. Figs. 2 and 3).

MTs of interphase control cells were horizontal and densely arranged (Fig. 4a), whereas of Cr-treated roots they appeared disordered and disoriented (Fig. 4b). In prophase cells of both the control (Fig. 4c) and the Cr-treated (Fig. 4d) roots a PPB of MTs and a perinuclear system were organized. However, in the Cr-treated the perinuclear system of MTs was disordered (Fig. 4d).

Metaphase cells of control roots developed the typical metaphase spindle consisting of MT bundles slightly

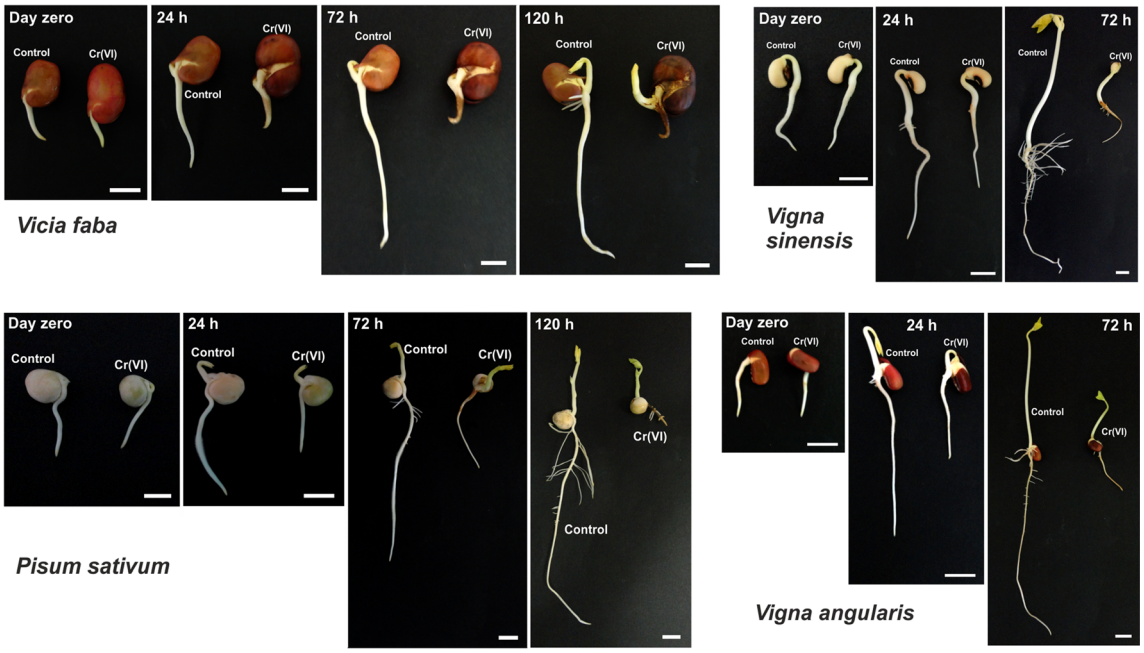

Fig. 1 Macroscopic effects of 250 μM Cr(VI) to seedlings used. All panels contain pairs of a control and a Cr-treated seedling at exposure times as depicted on the images. Seedlings of all species were severely affected by Cr(VI). *Bars* 1 cm

converging to broad poles and bore the chromosomes stringently positioned on the metaphase plate (Fig. 4e). The equivalent spindle of the Cr-treated cells contained fewer, short and vaguely defined MT bundles, while the chromosomes did not accumulate orderly on the metaphase plate (Fig. 4f). The anaphase spindle of control cells converged sharply to single poles, apparently drawing the daughter chromosomes to opposing poles (Fig. 4g). Unlikely, the anaphase spindle of Cr-treated cells contained many distinguishable and conical MT bundles converging to minipoles (Fig. 4h). Chromosomes of such cells were improperly separated and displayed several lagging arms.

During telophase, both the control and Cr-treated cells developed phragmoplasts symmetrically positioned between the newly formed nuclei (Fig. 4i, j). However, in the Cr-treated several lagging chromosome arms were noticed (Fig. 4j; cf. Fig. 4i).

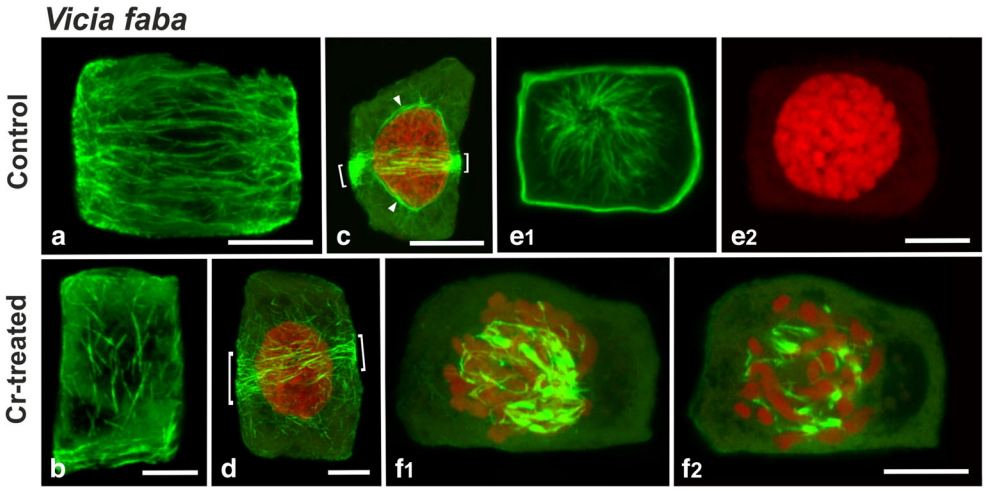

Fig. 2 *Vicia faba*, CLSM figures. **a** Control, interphase. The cortical MTs appear densely arranged, parallel to each other and horizontal relative to the vertical axis. **b** Cr-treated, interphase. The cortical MTs are disoriented and thinned out. **c** Control, prophase, *side view*. A narrow preprophase band (*PPB*) of MTs (*brackets*) encircles symmetrically the nucleus, which is surrounded by a prophase perinuclear system of MTs (*arrowheads*). **d** Cr-treated, prophase, *side view*. The PPB of MTs is not *narrowed* (*brackets*) and the perinuclear system of MTs is missing (cf. **c**). **e** Control, prophase, *top view*. The PPB of MTs is located at the cell periphery, the MTs of the perinuclear system form a radial cap ($\mathbf{e_1}$) on the *top* of the nucleus, which displays well condensed chromosomes ($\mathbf{e_2}$). **f** Cr-treated, prometaphase. Tubulin forms atypical masses around ($\mathbf{f_1}$) and among ($\mathbf{f_2}$) the chromosomes. $\mathbf{f_2}$ is a single central CLSM section of $\mathbf{f_1}$. *Bars* 10 μm

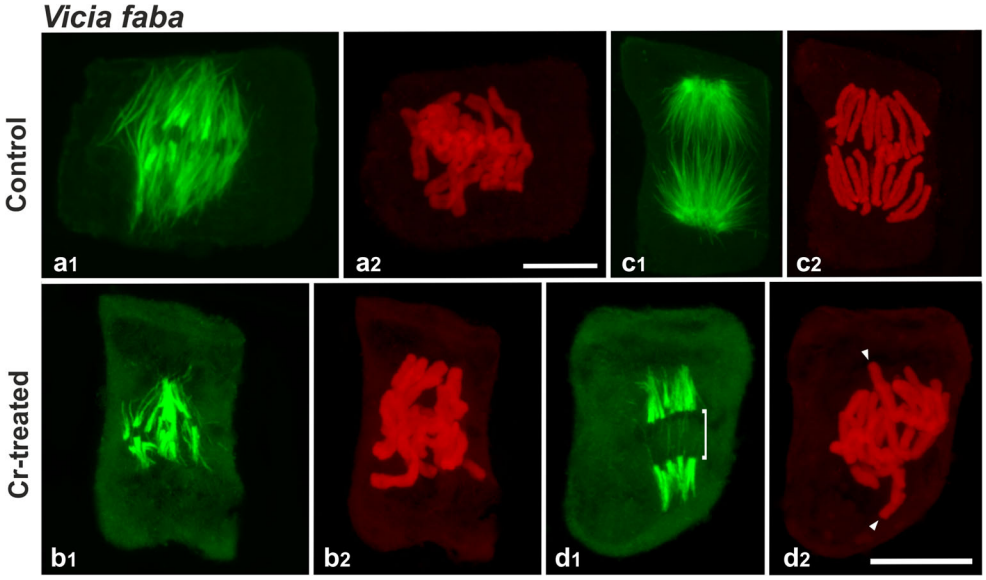

Fig. 3 *Vicia faba*, CLSM figures. **a** Control, metaphase. The spindle is symmetrical (**a_1**) and the chromosomes are arranged on the metaphase plate with their arms projecting (**a_2**). **b** Cr-treated, metaphase. The spindle is asymmetrical and consists of dense short tubulin bundles (**b_1**; cf. **a_1**), while the chromosomes are arranged atypically on the metaphase plate (**b_2**; cf. **a_2**). **c** Control, anaphase. The MTs of the anaphase spindle are shortened (**c_1**), the chromosomes well separated and being drawn to the poles (**c_2**). **d** Cr-treated, anaphase. The spindle MTs are condensed and leave a clear-cut in-between space (**d_1**, *bracket*; cf. **c_1**), while the chromosomes occur entangled in the cell centre with some projecting arms (**d_2**, *arrowheads*; cf. **c_2**). *Bars* 10 μm

Vigna sinensis

In control roots of *V. sinensis* interphase MTs displayed the typical parallel arrangement to each other, transversely aligned to the longitudinal axis of the root (Fig. 5a). Mid-prophase cells developed a narrow PPB of MTs at the central peripheral cytoplasm encircling symmetrically the nucleus, which moreover was outlined by a perinuclear system of MTs (Fig. 5b).

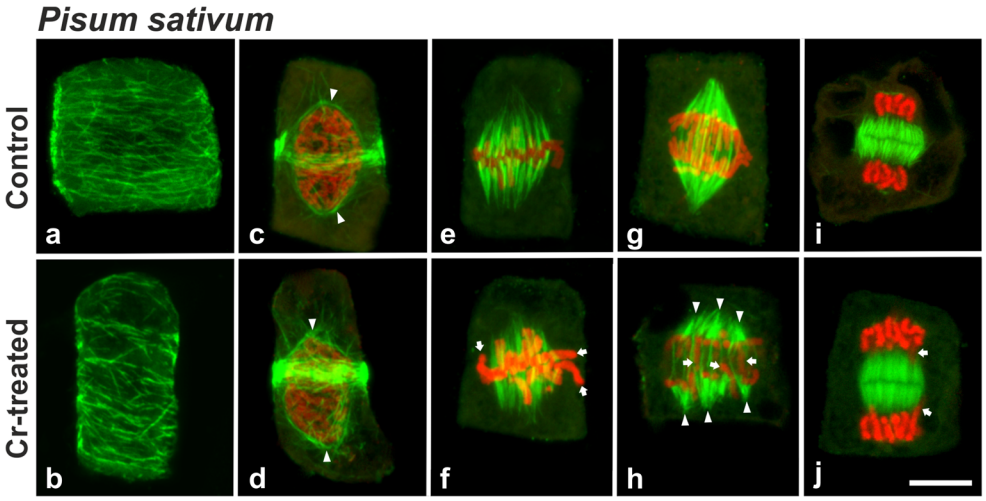

Fig. 4 *Pisum sativum*, CLSM figures. **a**, **b** Interphase. The cortical MTs are densely arranged parallel to each other and perpendicular to the longitudinal axis of the control cell (**a**), whereas in the Cr-treated they are slightly disordered and disoriented (**b**). **c**, **d** Prophase, control (**c**) and Cr-treated (**d**). A symmetrical PPB of MTs occurs at the equatorial plane and a perinuclear system of MTs (*arrowheads*) surrounds the nuclei of both cells. **e**, **f** Metaphase. In the control the mitotic spindle moieties converge slightly to broad poles being connected to the chromosomes arranged on the metaphase plate (**e**), while in the Cr-treated the spindle MTs are shorter and loosely defined among the chromosomes, which appear improperly aggregated on the metaphase plate (**f**, *arrows*). **g**, **h** Anaphase. The spindle MTs of the control converge strongly to single point poles and the chromosomes are well segregated being drawn to opposing directions (**g**). In the Cr-treated cell the anaphase spindle appears widened consisting of bundled MTs converging to multiple minipoles (**h**, *arrowheads*), while the chromosomes seem unequally drawn with many lagging arms (**h**, *arrows*). **i**, **j** Mid-telophase. The phragmoplast of the control cell is expanding symmetrically between the reforming nuclei (**i**), but in the Cr-treated cell the phragmoplast MTs appear indistinguishable from each other and the chromosome groups bear lagging arms (**j**, *arrows*). *Bar* 10 μm

Towards the end of prophase, the PPB of MTs diminished and disorganized, while the perinuclear system of MTs evolved to the prophase spindle, which was a bipolar apparatus encaging the nucleus and converging to the polar regions (Fig. 5c). Metaphase and anaphase cells developed normal metaphase and anaphase spindles with the chromosomes positioned on the metaphase plate (Fig. 5d) or the daughter chromatids being drawn towards the poles, respectively. Telophase cells contained two groups of well-separated chromosomes being organizing into the new nuclei on either side of a symmetrically extending phragmoplast (Fig. 5e).

In Cr-treated *V. sinensis* seedlings, dividing cells displayed severe and quite unusual abnormalities relative to the controls. Interphase MTs became perplexed, variously oriented (Fig. 5f) and in longer treatments (72 h) they formed dense entangled bundles (data not shown). In the prophase cells, both the PPB of MTs and the perinuclear MTs were disrupted: the PPBs were compact and rough, the perinuclear system was discontinuous and a fine network of MTs spread to the whole cytoplasm (Fig. 5g). The PPB of MTs disappeared in late prophase cells but the prophase spindle surrounding the nucleus lost its bipolar organization and displayed several minipoles in all directions (Fig. 5h). Cr-affected metaphase cells occupied abnormally positioned metaphase spindles, either integral or split in two or more components of unequal size (Fig. 5i). Moreover, metaphase spindle MTs were shorter than the control and chromosomes were not aggregated in a straight metaphase plate (Fig. 5i; cf. Fig. 5d). In top views, the metaphase plate of Cr-treated cells appeared lobed or indented (Fig. 5j). Anaphase spindles lost their vertical orientation and became oblique or diagonal, with the poles located very close to the cell periphery; anaphase chromosomes were incompletely segregated and ineffectively drawn to the poles, having many overlapping arms (Fig. 5k). Cr-treated telophase cells presented pronounced abnormalities (Fig. 5l–n). In top views, phragmoplasts displayed various atypical conformations ranging from heart-shaped (Fig. $5l_1$) to multi-segmented and branched ones (Fig. 5m, n), extending among many unequal groups of chromosomes (Fig. $5l_2$, n). In face views, phragmoplast segments were encountered not only at the equatorial plane but also at atypical locations of

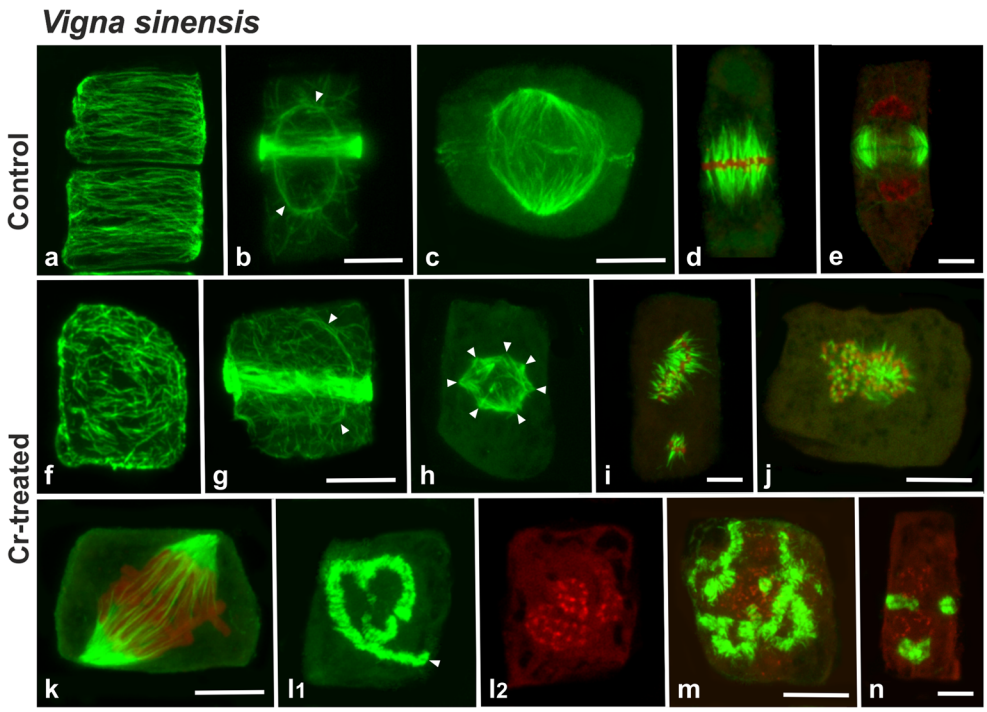

Fig. 5 *Vigna sinensis*, CLSM figures. **a**–**e** Controls. Interphase (**a**), prophase (**b**), late prophase (**c**), metaphase (**d**) and telophase (**e**) cells with typical arrays of mitotic MTs and chromosomes. *Arrowheads* in **b** point to the perinuclear MT network. **f**–**n** Cr-treated. **f** Interphase. MTs appear entangled and variously oriented. **g** Prophase. The PPB of MTs is compact and rough, while a dense reticulum of MTs delineates the nucleus outline (*arrowheads*) and extends to the whole cytoplasm. **h** Metaphase. The metaphase spindle has a polygonal shape with MTs converging to many atypical minipoles (*arrowheads*). **i**, **j** Metaphase cells, in *face* (**i**) and *top* (**j**) views. **j** is a single central CLSM section. The mitotic spindle in the *face view* appears diagonally oriented and split into a large and a small component (**i**), while in the *top view* it exhibits an unusual lobed shape (**j**). In both the spindle MTs intermingle with chromosomes. **k** Anaphase. The chromosomes have improperly been segregated by the diagonally oriented spindle. **l** Telophase, *top view*. $\mathbf{l_2}$ is a single central CLSM section. The phragmoplast has an unusual heart-like shape with a projecting arm ($\mathbf{l_1}$, *arrowhead*), extending among three unequal groups of chromosomes $\mathbf{l_2}$. **m** Multi-segmented, displaced and randomly oriented phragmoplast positioned among numerous small groups of chromosome aggregations. **n** Telophase, *face view*. The phragmoplast MTs form three atypical groups, while the chromosomes remain scattered in the cytoplasm. *Bars* 10 μm

the cytoplasm, overlapped with small non-segregated chromosome groups (Fig. 5n).

Vigna angularis

Interphase MTs of control cells of *V. angularis* displayed the typical parallel orientation, transversely aligned to the long axis of the root (Fig. 6a). Unlikely, in the Cr-treated cells cortical MTs became highly bundled, elongated, wavy and obliquely oriented (Fig. 6b). The PPB of MTs of prophase cells of untreated roots engirdled symmetrically the nuclei, which were shrouded by the mirrored caps of prophase spindle (Fig. 6c). These prophase MT arrays were severely disrupted in the respective prophase cells of Cr-treated roots as the PPB of MTs was discontinuous and compact, while the prophase spindle MTs were randomly aligned and perplexed around the nuclei and the cytoplasm (Fig. 6d).

The metaphase spindles of both the control (Fig. 6e) and Cr-treated (Fig. 6f) cells were morphologically similar, but a closer view revealed that the straight positioning of chromosomes of the control metaphase plate in the Cr-treated became zigzagged (Fig. 6f; cf. Fig. 6e).

Control anaphase cells contained the normal anaphase spindle (Fig. 6g), whereas anaphase spindles of the Cr-treated cells appeared compact, disoriented and asymmetric, intermingled with unsegregated chromosomes (Fig. 6h). Finally, untreated telophase cells bore symmetrical phragmoplasts expanding between the two groups of daughter chromosomes developing into the new nuclei (Fig. 6i), in contrast to Cr-treated cytokinetic cells that contained segmented phragmoplasts and several groups of chromosomes of unequal size (Fig. 6j).

Discussion

Members of the Fabaceae family have for long been used to decipher several aspects of Cr toxicity in plants, occasionally in comparison with other metals. Such studies revealed suppressive effects to both seed germination and root growth (Parr and Taylor 1982; Bishnoi et al. 1993; Rout et al. 1997; Peralta et al. 2001; Zeid 2001; Samantary 2002; Jamal et al. 2006). The ability of seeds to germinate in the presence of Cr may be indicative of tolerance. For instance, Peralta et al. (2001) showed that 40 ppm Cr(VI) diminished seed germination of *Medicago sativa* stronger than cadmium, copper, nickel and zinc, and was one of the most suppressive to shoot and root growth, confirming its high phytotoxicity at elevated concentrations. Moreover, Cr(VI) suspended lateral root development in Cr-sensitive cultivars of *Vigna radiata* more than in Cr-tolerant ones (Samantary 2002).

The prejudicial effects of Cr(VI) to the seedlings currently investigated were readily visualized by the reduced or inhibited growth of the roots and shoots, as well as by the browning of the roots. Root darkening is a usual symptom of

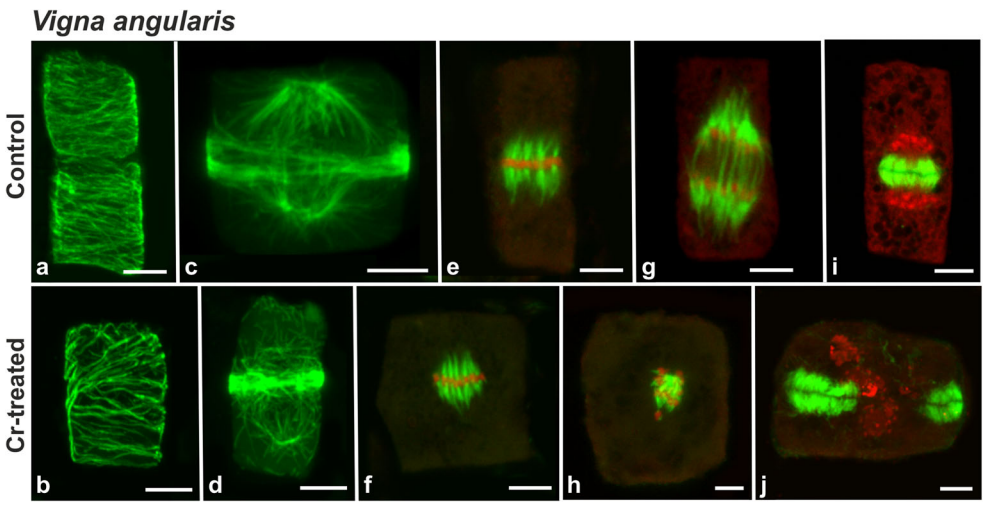

Fig. 6 *Vigna angularis*, CLSM figures. **a**, **b** Interphase. The cortical MTs of the control cells are parallel to each other and perpendicular to the longitudinal axis (**a**), while in the Cr-treated one they are bundled, elongated, wavy and obliquely oriented (**b**). **c**, **d** Prophase. The PPB of MTs of the control cell girdles the nucleus and the prophase spindle encages it like two mirrored caps (**c**). In the Cr-treated cell the PPB of MTs is compact and discontinuous, while the prophase spindle is destroyed with the MTs randomly positioned (**d**). **e**, **f** Metaphase. The metaphase spindle of the control consists of short moieties terminating at the chromosomes aggregated on the metaphase plate (**e**), in the Cr-treated it appears almost normal but the chromosomes are zigzagged located on the metaphase plate (**f**). **g**, **h** Anaphase. The control spindle is contracted and the chromosomes are being drawn to the poles (**g**), whereas the Cr-treated one is compact, disoriented, asymmetric and overlapping with scattered chromosomes (**h**). **i**, **j** Telophase. The phragmoplast of the control cell extends between the separated chromosome groups (**i**), of the Cr-treated it is split into two unequal segments, while the chromosomes are accumulated in at least three groups (**j**). *Bars*: 10 μm

Cr (Bianchi et al. 1998; Mallick et al. 2010) and of other metals (Adamakis et al. 2008) toxicity. Reduction in germination of Cr-treated seeds of *Phaseolus vulgaris* was attributed to the depressive effects of Cr on the activity of amylases and concomitantly the enhancement of protease activity (Zeid 2001). Moreover, decrease or complete suspension of root growth under Cr(VI) exposure may be explained by inhibition of cell divisions (current study), combined with tissue collapse and incapacity of the roots to absorb water and nutrients from the medium (Barceló et al. 1985).

The decline of root and the whole seedling growth after exposure to Cr(VI) was consistently reflecting the disturbance of MT arrays in all species investigated, favouring the view that MTs may constitute a prime universal target of Cr toxicity. This conclusion was previously suggested for *P. sativum* exposed to cadmium (Fusconi et al. 2007) and was shown in taxonomically diverse land plant taxa exposed to tungsten (Adamakis et al. 2010b). It is then tempting to generalize that MTs might constitute a sensitive, reliable and universal cellular marker for monitoring heavy metal toxicity in higher plants.

Different metals (cadmium, lead, nickel, aluminium and copper) have affected differentially the MT organization of a single species (Dovgalyuk et al. 2003; Malea et al. 2013). The reverse question, that is the putative differential response of MTs of different plant species to a given heavy metal, has hitherto attracted little attention and is restricted to the differential effects of tungsten on representative land plant taxa (Adamakis et al. 2010b) and of Cr(VI) on *A. cepa* (Eleftheriou et al. 2012) and *L. culinaris* (Eleftheriou et al. 2013). Divergent effects have even been reported for various MT arrays of a given species treated with a single metal. For instance, in *Zea mays*, the transverse interphase MTs and mitotic spindles were more sensitive to lead than other MT arrays (Eun et al. 2000). Similar inter-array differences have also been observed in the current study, which extends the range of plant species searched under this context and reveals differential reaction (depolymerization versus bundling) of the mitotic MT arrays among four different yet related species to Cr(VI), suggesting a species-specific response to the same phytotoxic factor.

Irrespective whether mitotic MT arrays were depolymerized or bundled after exposure to Cr(VI), the result was fatal for the cell cycle: failure of chromosomes to aggregate on the metaphase plate, to segregate and move to opposing poles at anaphase and to form the new nuclei at telophase, while cytokinesis was dramatically disrupted. The chromosomal aberrations frequently reported in the literature in diverse plant species exposed to Cr stress (see "Introduction") are herewith confirmed. Moreover, it is shown that in the species investigated they are underlain by MT impairment, an effect that might have occurred as well in the other studies reporting chromosomal abnormalities and where MTs were not visualized (Knasmüller et al. 1998; Wang 1999; Qian 2004; Truta et al. 2014). Vigorously dividing cells of the apical root meristems, deprived of functional MTs, were blocked from further progress and aberrant images were produced depending on the accurate stage the cells were found at the time of Cr(VI) entrance, similarly to the effects of other metals in dividing plant cells (Frantzios et al. 2000, 2001). The atypical small groups of chromosomes observed at telophase (Figs. 5l$_2$, m, n and 6j) would apparently produce micronuclei, which are frequently used to detect cytotoxic and genotoxic damage induced by environmental pollutants, including Cr (Degrassi and Rizzoni 1982; Ma et al. 1995; Knasmüller et al. 1998; Wang 1999; Qian 2004). Should the formation of these vagrant chromosomes be the result of MT derangement, the view that MTs could be a quicker cellular diagnostic feature than other effects such as the formation of micronuclei and cell death is further substantiated (Fusconi et al. 2007; Eleftheriou et al. 2013; Malea et al. 2013).

The disorders of chromosome cycle induced by Cr(VI) are reminiscent of those caused by anti-MT agents (see "Introduction"). Presumably Cr(VI) affects MTs in a similar way. Mitotic MTs of *V. faba* seemed to have been depolymerized in almost all mitotic phases (Figs. 2 and 3), of *P. sativum* they were less deranged and appeared at normal locations (Fig. 4), while in *V. sinensis* and *V. angularis* they were severely disrupted, bundled or replaced by atypical tubulin conformations (Figs. 5 and 6). Recently, it was shown that in *L. culinaris*, another Fabaceae member, Cr(VI)-induced bundled MTs were highly acetylated (Eleftheriou et al. 2013). Tubulin acetylation is a post-translational modification serving as a marker for stable MTs (Perdiz et al. 2011). Whether bundling of cortical MTs in the species herewith investigated is correlated with elevated MT acetylation is the subject of another parallel research.

Conclusions

Evidence obtained in the present study favours the view that mitotic MTs constitute a prime subcellular and universal target of Cr(VI) toxicity in plant cells, rendering them a sensitive, reliable and quick cellular marker for monitoring heavy metal toxicity. However, MTs of the four taxonomically related species investigated in this study were affected differentially since they were depolymerized or bundled, indicative of species-specific response to the same phytotoxic factor. Irrespective, severe aberrations of mitosis and cytokinesis were incurred, leading to the conclusion that the abnormalities of chromosomal cycle are mediated by the disturbance of the corresponding MT arrays. Although MTs may primarily manifest the detrimental effects of Cr(VI) in plant cells, we cannot yet explain the precise mechanism governing this phenomenon. Moreover, considering that acetylated *a*-tubulin levels

may change after Cr(VI) treatment (Eleftheriou et al. 2013), it is motivating to clarify the acetylation status of MTs in the species investigated.

Acknowledgments This research was financially supported by the Department of Botany, School of Biology, Aristotle University of Thessaloniki, Greece. We are grateful to Dr. Anastasia Tsingotjidou, Faculty of Veterinary Medicine, Aristotle University of Thessaloniki, Greece, for generously providing access to the Nikon D-Eclipse C1 CLSM, and to Dr. Takahiro Hamada (Kyoto University, Japan) for cordially providing seeds of *V. angularis*.

References

Adamakis I-DS, Eleftheriou EP, Rost TL (2008) Effects of sodium tungstate on the ultrastructure and growth of pea (*Pisum sativum*) and cotton (*Gossypium hirsutum*) seedlings. Environ Exp Bot 63: 416–425

Adamakis I-DS, Panteris E, Eleftheriou EP (2010a) Tungsten affects the cortical microtubules of *Pisum sativum* root cells: experiments on tungsten-molybdenum antagonism. Plant Biol 12:114–124

Adamakis I-DS, Panteris E, Eleftheriou EP (2010b) The cortical microtubules are a universal target of tungsten toxicity among land plant taxa. J Biol Res (Thessaloniki) 13:59–66

Adamakis I-DS, Panteris E, Eleftheriou EP (2011) The fatal effect of tungsten on *Pisum sativum* L. root cells: indications for endoplasmic reticulum stress-induced programmed cell death. Planta 34:21–34

Barceló J, Poschenriender C, Ruano A, Gunse B (1985) Leaf water potential in Cr(VI) treated bean plants (*Phaseolus vulgaris* L). Plant Physiol Suppl 77:163–164

Bianchi A, Corradi MG, Tirillini B, Albasini A (1998) Effects of hexavalent chromium on *Mentha aquatica* L. J Herbs Spices Med Plants 5:3–12

Bishnoi NR, Dua A, Gupta VK, Sawhney SK (1993) Effect of chromium on seed germination, seedling growth and yield of peas. Agric Ecosyst Environ 47:47–57

Botsou F, Karageorgis AP, Dassenakis E, Scoullos M (2011) Assessment of heavy metal contamination and mineral magnetic characterization of the Asopos River sediments (Central Greece). Marine Poll Bull 62:547–563

Degrassi F, Rizzoni M (1982) Micronucleus test in *Vicia faba* root tips to detect mutagen damage in fresh-water pollution. Mut Res 97:19–23

Dho S, Camusso W, Mucciarelli M, Fusconi A (2010) Arsenate toxicity on the apices of *Pisum sativum* L. seedling roots: effects on mitotic activity, chromatin integrity and microtubules. Environ Exp Bot 69: 17–23

Dovgalyuk A, Kalynyak T, Blume YB (2003) Heavy metals have a different action from aluminium in disrupting microtubules in *Allium cepa* meristematic cells. Cell Biol Intern 27:193–195

EC Council Directive (98/83/EC) of 3 November 1998 on the quality of water intended for human consumption. Official J Eur Comm L330/32

Economou-Eliopoulos M, Megremi I, Vasilatos C (2011) Factors controlling the heterogeneous distribution of Cr(VI) in soil, plants and groundwater: evidence from the Assopos basin, Greece. Chem Erde 71:39–52

Eleftheriou EP, Adamakis I-DS, Melissa P (2012) Effects of hexavalent chromium on microtubule organization, ER distribution and callose deposition in root tip cells of *Allium cepa* L. Protoplasma 249:401–416

Eleftheriou EP, Adamakis I-DS, Fatsiou M, Panteris E (2013) Hexavalent chromium disrupts mitosis by stabilizing microtubules in *Lens culinaris* Moench. root tip cells. Physiol Plant 147:169–180

Eun S-O, Youn HS, Lee Y (2000) Lead disturbs microtubule organization in the root meristem of *Zea mays*. Physiol Plant 110:356–365

Frantzios G, Galatis B, Apostolakos P (2000) Aluminium effects on microtubule organization in dividing root-tip cells of *Triticum turgidum*. I. Mitotic cells. New Phytol 145:211–224

Frantzios G, Galatis B, Apostolakos P (2001) Aluminium effects on microtubule organization in dividing root-tip cells of *Triticum turgidum*. II. Cytokinetic cells. J Plant Res 114:157–170

Fusconi A, Gallo C, Camusso W (2007) Effects of cadmium on root apical meristems of *Pisum sativum* L.: cell viability, cell proliferation and microtubule pattern as suitable markers for assessment of stress pollution. Mut Res 632:9–19

Hepler P, Hush JM (1996) Behavior of microtubules in living plant cells. Plant Physiol 112:455–461

Hu Y, Liu X, Bai J, Shih K, Zeng EY, Cheng H (2013) Assessing heavy metal pollution in the surface soils of a region that had undergone three decades of intense industrialization and urbanization. Environ Sci Pollut Res 20:6150–6159

Jamal SN, Iqbal MZ, Athar M (2006) Effect of aluminum and chromium on the germination and growth of two *Vigna* species. Int J Environ Sci Tech 3:53–58

Kimbrough DE, Cohen Y, Winer AM, Creelman L, Mabuni C (1999) A critical assessment of chromium in the environment. Crit Rev Environ Sci Technol 29:1–46

Kirkillis CG, Pasias IN, Miniadis-Meimaroglou S, Thomaidis NS, Zabetakis I (2012) Concentration levels of trace elements in carrots, onions, and potatoes cultivated in Asopos region, Central Greece. Anal Lett 45:551–562

Knasmüller S, Gottmann E, Steinkellner H, Fomin A, Pickl C, Paschke A, Göd R, Kundi M (1998) Detection of genotoxic effects of heavy metal contaminated soils with plant bioassays. Mut Res 420:37–48

Labra M, Grassi F, Imazio S, Di Fabio T, Citterio S, Sgorbati S, Agradi E (2004) Genetic and DNA-methylation changes induced by potassium dichromate in *Brassica napus* L. Chemosphere 54:1049–1058

Liu D, Xue P, Meng Q, Zou J, Gu J, Jiang W (2009) Pb/Cu effects on the organization of microtubule cytoskeleton in interphase and mitotic cells of *Allium sativum* L. Plant Cell Rep 28:695–702

Liu J, Zhang X-H, Tran H, Wang D-Q, Zhu Y-N (2013) Heavy metal contamination and risk assessment in water, paddy soil, and rice around an electroplating plant. Environ Sci Pollut Res 18:1623–1632

Ma T-H, Xu Z, Xu C, McConnell H, Rabago EV, Arreola GA, Zhang H (1995) The improved *Allium*/*Vicia* root tip micronucleus assay for clastogenicity of environmental pollutants. Mut Res 334:185–195

Malea P, Adamakis I-DS, Kevrekidis T (2013) Microtubule integrity and cell viability under metal (Cu, Ni and Cr) stress in the seagrass *Cymodocea nodosa*. Chemosphere 93:1035–1042

Mallick S, Sinam G, Kumar Mishra R, Sinha S (2010) Interactive effects of Cr and Fe treatments on plants growth, nutrition and oxidative status in *Zea mays* L. Ecotoxicol Environ Safety 73:987–995

Morejohn LC (1991) The molecular pharmacology of plant tubulin and microtubules. In: Lloyd CW (ed) The cytoskeletal basis of plant growth and form. Academic, London, pp 29–43

Oliveira H (2012) Chromium as an environmental pollutant: insights on induced plant toxicity. J Bot 2012: ID375843, 8p

Parr PD, Taylor FG Jr (1982) Germination and growth effects of hexavalent chromium in Orocol TL (a corrosion inhibitor) on *Phaseolus vulgaris*. Environ Int 7:197–202

Peralta JR, Gardea-Torresdey JL, Tiemann KJ, Gomez E, Arteaga S, Rascon E, Parsons JG (2001) Uptake and effects of five heavy metals on seed germination and plant growth in alfalfa (*Medicago sativa* L.). Bull Environ Contam Toxicol 66:727–734

Perdiz D, Mackeh R, Pous C, Baillet A (2011) The ins and outs of tubulin acetylation: more than just a post-translational modification? Cell Signal 23:763–771

Qian X (2004) Mutagenic effects of chromium trioxide on root tip cells of *Vicia faba*. J Zhejiang Univ (Sci) 5:1570–1576

Rodriguez E, Azevedo R, Fernandes P, Santos C (2011) Cr(VI) induces DNA damage, cell cycle arrest and polyploidization: a flow cytometric and comet assay study in *Pisum sativum*. Chem Res Toxicol 24:1040–1047

Rout GR, Samantaray S, Das P (1997) Differential chromium tolerance among eight mungbean cultivars grown in nutrient culture. J Plant Nutr 20:473–483

Samantary S (2002) Biochemical responses of Cr-tolerant and Cr-sensitive mung bean cultivars grown on varying levels of chromium. Chemosphere 47:1065–1072

Singh HP, Mahajan P, Kaur S, Batish DR, Kohli RK (2013) Chromium toxicity and tolerance in plants. Environ Chem Lett 13:229–254

Speranza A, Ferri P, Battistelli M, Falcieri E, Crinelli R, Scoccianti V (2007) Both trivalent and hexavalent chromium strongly alter *in vitro* germination and ultrastructure of kiwifruit pollen. Chemosphere 66: 1165–1174

Speranza A, Taddei AR, Gambelini G, Ovidi E, Scoccianti V (2009) The cell wall of kiwifruit pollen tubes is a target for chromium toxicity: alterations to morphology, callose pattern and arabinogalactan protein distribution. Plant Biol 11:179–193

Truta E, Mihai C, Gherghel D, Vochita G (2014) Assessment of the cytogenetic damage induced by chromium short-term exposure in root tip meristems of barley seedlings. Water Air Soil Poll 225:1993. doi:10.1007/s11270-014-1933-x

Tziritis E, Kelepertzis E, Korres G, Perivolaris D, Repani S (2012) Hexavalent chromium contamination in groundwaters of Thiva basin. Cent Greece Bull Environ Contam Toxicol. doi:10.1007/s00128-012-0831-4

van der Vaart B, Akhmanova A, Straube A (2009) Regulation of microtubule dynamic instability. Biochem Soc Trans 37:1007–1013

Vázquez MD, Poschenrieder C, Barceló J (1987) Chromium VI induced structural and ultrastructural changes in bush bean plants (*Phaseolus vulgaris* L.). Ann Bot 59:427–438

Wang H (1999) Clastogenicity of chromium contaminated soil samples evaluated by *Vicia* root-micronucleus assay. Mutat Res 426:147–149

Wick SM (1985) Immunofluorescence microscopy of tubulin and microtubule arrays in plant cells. III. Transition between mitotic/cytokinetic and interphase microtubule arrays. Cell Biol Intern Rep 9:357–371

Xu P, Liu D, Jiang W (2009) Cadmium effects on the organization of microtubular cytoskeleton in interphase and mitotic cells of *Allium sativum*. Biol Plant 53:387–390

Zeid IM (2001) Responses of *Phaseolus vulgaris* to chromium and cobalt treatments. Biol Plant 44:111–115